arXiv:2212.13736v1 [cond-mat.mes-hall] 28 Dec 2022

Hermitian Topologies originating from non-Hermitian braidings

W. B. Rui,[1] Y. X. Zhao,[2,3,*] and Z. D. Wang[1,†]

[1] *Department of Physics and HKU-UCAS Joint Institute for Theoretical and Computational Physics at Hong Kong, The University of Hong Kong, Pokfulam Road, Hong Kong, China*

[2] *National Laboratory of Solid State Microstructures and Department of Physics, Nanjing University, Nanjing 210093, China*

[3] *Collaborative Innovation Center of Advanced Microstructures, Nanjing University, Nanjing 210093, China*

(Dated: December 29, 2022)

The complex energy bands of non-Hermitian systems braid in momentum space even in one dimension. Here, we reveal that the non-Hermitian braiding underlies the Hermitian topological physics with chiral symmetry under a general framework that unifies Hermitian and non-Hermitian systems. Particularly, we derive an elegant identity that equates the linking number between the knots of braiding non-Hermitian bands and the zero-energy loop to the topological invariant of chiral-symmetric topological phases in one dimension. Moreover, we find an exotic class of phase transitions arising from the critical point transforming different knot structures of the non-Hermitian braiding, which are not included in the conventional Hermitian topological phase transition theory. Nevertheless, we show the bulk-boundary correspondence between the bulk non-Hermitian braiding and boundary zero-modes of the Hermitian topological insulators. Finally, we construct typical topological phases with non-Hermitian braidings, which can be readily realized by artificial crystals.

I. INTRODUCTION

The concept of topology captures properties unchanged under continuous deformations. It can be pictorially illustrated by knots formed by braids, which cannot be unknotted by continuous stretching. While initially introduced to describe the behavior of anyons [1–3], braiding was recently actively investigated in momentum-space band structures [4–19], where braids appear in various scenes, such as nodal lines in topological semimetals [4–7], the trajectories of Weyl or Dirac points in adiabatic time evolution [8–11], and exceptional rings in non-Hermitian systems [12–15].

Another active trend in recent research is to generalize elements of Hermitian topological phases to non-Hermitian systems [20–34]. Fundamental topological concepts, such as topological invariants, bulk-boundary correspondence, and topological stability, were reconsidered by incorporating non-Hermitian features [30, 32–39], such as gain-and-lose processes and exceptional points. This leads to novel topological classifications, and a plethora of non-Hermitian topological phase with exotic non-Hermitian topological phemonena [30, 32–53]. Particularly, massive number of states reside on the boundary in the non-Hermitian skin effect [47–54], rather than a few boundary states for Hermitian topological insulators.

Non-Hermitian physics and braiding are not independent. The energy spectra of non-Hermitian systems are complex numbers, and hence the complex bands can naturally braid in the complex plane even through a 1D Brillouin zone. This leads to a recent classification of non-Hermitian 1D systems by the knot structures [55–59].

In this article, we reverse the conventional reasoning by understanding Hermitian topological physics in terms of non-Hermitian braiding in one dimension. *A priori*, there is a formal one-to-one map between a Hermitian Hamiltonian H in class AIII and a non-Hermitian operator Q in the basis specified by the eigenstates of the chiral symmetry. Using the map, we find that a number of fundamentals of Hermitian topology acquire more pictorial understandings from the braiding structure of the non-Hermitian bands. Particularly, we rigorously show that the abstractly defined topological invariant of the Su-Schrieffer-Heeger (SSH) model can be visualized as the linking number between the knots of the complex non-Hermitian bands and the zero-energy loop. Since the left and right zero-modes of Q are exactly the zero modes of H with opposite chirality, we see that the end zero modes of the Hermitian insulator can be regarded as consequences of the bulk non-Hermitian braiding. Nevertheless, the braiding rationale can give rise to a novel class of topological phase transitions characterized by the critical points where the knot structure of the non-Hermitian bands transforms, which go beyond the conventional theory of topological phase transitions. Moreover, we construct typical topological phases using our theory, which can be readily realized by artificial crystals.

II. FRAMEWORK

Let us start with a non-Hermitian system described by the Hamiltonian Q. Using Q, a Hermitian Hamiltonian H with chiral symmetry S can be built as

$$H=\begin{pmatrix}0 & Q\\ Q^\dagger & 0\end{pmatrix},\quad S=\begin{pmatrix}\mathbb{I} & 0\\ 0 & -\mathbb{I}\end{pmatrix},\quad SHS^\dagger=-H. \tag{1}$$

* zhaoyx@nju.edu.cn
† zwang@hku.hk

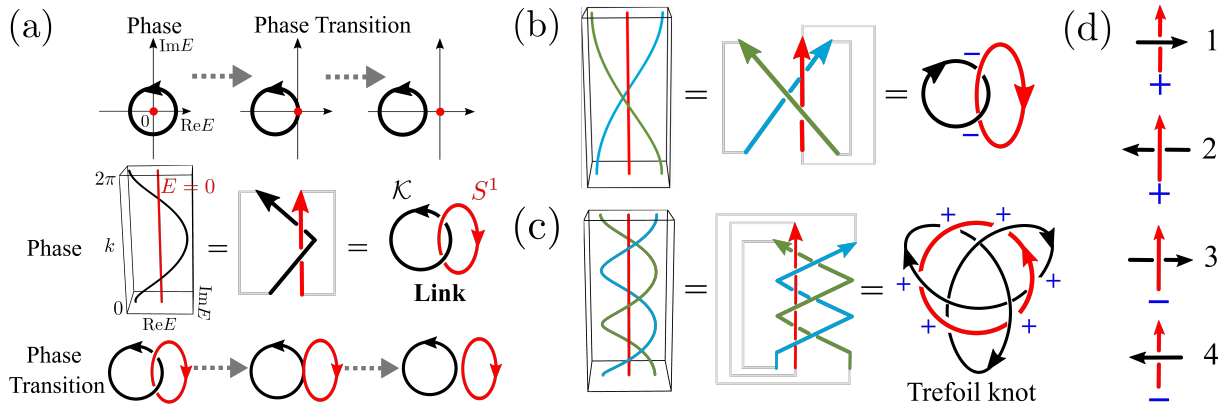

Fig. 1. Non-Hermitian braidings as the origin of Hermitian topological phases. (a) Upper panel: the conventional 2D picture of topological phase and its transition. Middle panel: The single band braids trivially and forms a knot of circle. The 3D picture shows the topological origin as the linking between knot (black) and zero-energy loop (red). Lower panel: 3D picture of unlinking as the phase transition. (b) Knot of circle formed by the braiding of bands. (c) Trefoil knot formed by the braiding of bands. (d) Illustrations of four types of crossings in the algorithm to calculate the topological invariant.

Here † denotes the conjugate transpose and $\mathbb{I}$ the identity matrix. For the eigenequtions $H|\Psi\rangle = E|\Psi\rangle$, the chiral symmetry results in another set of eigenmodes $\{-E, S|\Psi\rangle\}$. Thus, the energy spectrum is symmetric with respect to zero energy.

A key observation is that for zero energy, i.e., $E = 0$, the chiral-symmetric Hermitian H is decoupled to non-Hermitian Q and $Q^\dagger$. Though seemingly minor, we will show that the non-Hermitian topological properties of Q with respect to this zero energy dictate the bulk topology, topological phase transition, and bulk-boundary correspondence of the Hermitian H. Thus, the zero energy serves as a guideline in our study.

Since zero-energy eigenstates of H are at the same time the eigenstates of S, they can be classified as left-handed (right-handed) according to the eigenvalues $+1(-1)$ of the chiral operator. Introduce $|\Psi\rangle = (\psi_+, \psi_-)^T$ as the eigenstates of H. The zero-energy eigenstates ($|\Psi_\pm\rangle$) of different chiralities are obtained as

$$H|\Psi_\pm\rangle = 0: \quad |\Psi_+\rangle = (\psi_+, 0)^T, |\Psi_-\rangle = (0, \psi_-)^T, \quad (2)$$

which satisfies $S|\Psi_\pm\rangle = \pm|\Psi_\pm\rangle$. Clearly, H shares the same eigenstates with Q and $Q^\dagger$, as

$$E = 0: \quad Q^\dagger\psi_+ = 0, \quad Q\psi_- = 0. \quad (3)$$

Thus, we may regard that the zero-energy modes in chiral-symmetric Hermitian systems originate from the non-Hermitain components. In contrast, non-zero-energy eigenstates of Q can not retain in H [60].

III. ORIGIN OF HERMITIAN TOPOLOGICAL PHASES: BRAIDINGS OF NON-HERMITIAN ENERGY BANDS

We consider Q with no symmetry (non-Hermitian class A) and H with only chiral symmetry (Hermitian class AIII) in Eq. (1) [32, 61]. In one dimension (1D), both H and Q are characterized by the winding number of

$$w = \frac{1}{2\pi i}\oint_{\mathrm{BZ}^1} dk \cdot \nabla_k \log\det \mathcal{Q}(k), \quad (4)$$

where k denotes the momentum and $\mathcal{Q}(k)$ the corresponding Hamiltonian in the 1D Brillouin zone (BZ^1) [62, 63]. In this regard, $H(k)$ and $Q(k)$ share the same topology, and formerly, correspondences between the two have been established [30, 32, 64, 65]. It turns out the "one-to-one correspondence" [32, 64] describing the topological equivalence between the Hermitian topology of H and the point-gap topology [66] of Q is quite useful, and a systematic classification of the point-gap topology of Q using H has been worked out in higher dimensions and in other symmetry classes.

It shall be noted that the "one-to-one correspondence" above is based on the point-gap topology of Q. Recently, however, it has been shown that the non-Hermitian $\mathcal{Q}(k)$ actually has a 3D braiding topology in the (k, ReE, ImE)-space [55–58] as shown in Figs. 1(a,b,c), which goes beyond the point-gap topology. In view of this, the well-established equivalence relation between Q and H may not be sufficient.

However, the topological invariant in Eq. (4) is not able to capturing all the essential physics, because it is essentially a 2D quantity, while the braiding structure of $Q(k)$ lives in 3D. Thus, it is necessary to develop a 3D picture to understand the topological origin and the relation between Q and H. In the middle panel of Fig. 1(a), the single band of $\mathcal{Q}(k)$ braids trivially and forms a knot of circle (black) over BZ in 3D, while the zero-energy point forms a closed loop (red). To have a non-trivial phase, the knot ($\mathcal{K}$) and the zero-energy loop (S^1) must form a link. Note that the zero-energy loop S^1 is defined by a constant function $E(k) = 0$, which forms a loop due the periodicity of BZ. Then, the winding number

in Eq. (4) actually reflects the linking number between the two,

$$w = \mathrm{Link}(\mathcal{K}, S^1). \tag{5}$$

It is clear now that the topological phase transition, as shown in the lower panel of Fig. 1(a), is triggered by the unlinking process between $\mathcal{K}$ and S^1. This is in contrast with the conventional understanding of the phase transition induced by shifting the energy band away from the zero-energy point, as shown by the upper panel of Fig. 1(a).

The linking number of Eq. (5) goes beyond the previously mentioned correspondence between $\mathcal{H}(k)$ and $\mathcal{Q}(k)$, and can faithfully describe the topological origin of $\mathcal{H}(k)$. This is more evident for general cases of multi-band $\mathcal{Q}(k)$. In these cases, the n separable bands of $\mathcal{Q}(k)$ braid with each other [e.g., Figs. 1(b, c)], and form knots due to the periodicity of BZ. As different braiding structures may correspond to the same point-gap topology, the 2D winding number by Eq. (4), while valid in describing point-gap topology, may be blind to these 3D braiding structures. The 3D linking number, on the other hand, can faithfully tell us that the topological phases of $\mathcal{H}(k)$ originate from the non-Hermitian braidings in $\mathcal{Q}(k)$.

Compared to Eq. (4), the linking number may also simplify the calculation [67], because it can be obtained by just counting the crossings,

$$\mathrm{Link}(\mathcal{K}, S^1) = \frac{n_1 + n_2 - n_3 - n_4}{2}, \tag{6}$$

where n_i denotes the number of four types of crossings, as shown in Fig. 1(d). For instance, by simply counting the crossings, the winding number of the knot of circle in (b) and the Trefoil knot in (c) is obtained as $w = -1$ and $+3$, respectively.

IV. HERMITIAN TOPOLOGICAL PHASE TRANSITION VIA CRITICAL POINT IN NON-HERMITIAN BRAIDINGS

The above discussion of the non-Hermitian braidings as the origin of Hermitian topology leads to our discovery of a novel kind of topological phase transitions, which goes beyond the conventional theory of topological phase transitions shown in the first row of Fig. 1(a).

As illustrated by Fig. 2(a), where the two bands braid with each other, the linking number can also be changed by the transformation of the braiding structure. Here, the unlinking between $\mathcal{K}$ and S^1 is realized by the change of braiding of $\mathcal{Q}(k)$. It happens via the critical point where two bands intersect on the zero-energy loop. Such a critical point is a unique non-Hermitian degeneracy, namely, exceptional point (EP) [26, 57], which results in the phase transition in $\mathcal{H}(k)$.

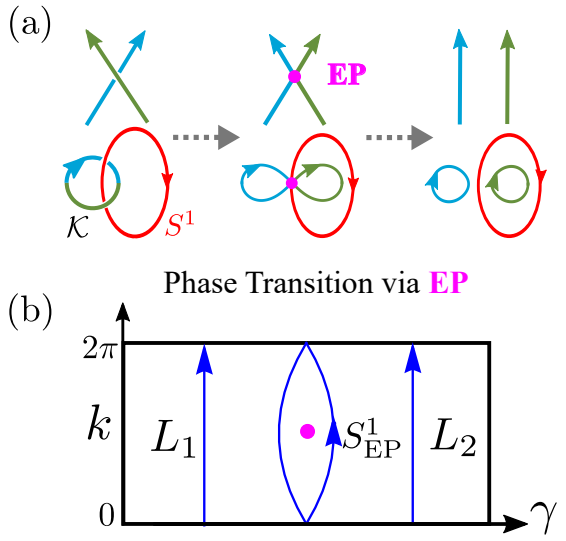

Fig. 2. (a) The transformation of non-Hermitian braiding in $\mathcal{Q}(k)$ via EP. (b) The transformation via EP can induce Hermitian topological phase transition in $\mathcal{H}(k)$.

To show that EPs can induce phase transition in Hermitian systems, recall that for order-2 EPs in 2D space, there is an associated topological invariant of of vorticity [26, 68]

$$v_{\pm} = -\frac{1}{2\pi}\oint_{S^1_{\mathrm{EP}}} dk \cdot \nabla_k \ \arg\left[E_+(k) - E_-(k)\right], \tag{7}$$

where $\pm$ denote the band indices, and S^1_{EP} is a 1D circle that goes around an exceptional point at the position k_{EP} in this 2D space, as shown in Fig. 2(b). The vorticity is a non-Hermitian invariant and takes half integer values ($\mathbb{Z}/2$), because EP acts as a branch point on the complex-energy plane. Thus, it is essentially different from Hermitian topological invariants.

Notably, it can be proved that EP can alter the winding number of

$$w(k_{\mathrm{EP}}) = \frac{1}{2\pi i}\oint_{S^1_{\mathrm{EP}}} dk \cdot \nabla_k \log\det \mathcal{Q}(k), \tag{8}$$

by $w(k_{\mathrm{EP}}) = -2v_{\pm}$. The derivation details can be found in the Supplemental Materials (SM) [69]. Thus, even though EP and its topological invariant are essentially non-Hermitain, it can determine Hermitian phase transition, and such a phase transition is different conventional ones as shown in Fig. 1(a) by shifting energies.

Let us return to the 1D systems. By treating one of the two dimensions as the parameter to control the phase transition, e.g, $\mathbf{k} \to \{k, \gamma\}$ in Fig. 2(b), the above topological invariant signifies the transition of topological phases in 1D. Because due to topological robustness, the circle S^1_{EP} can be deformed to two loops, L_1 and L_2, as shown in Fig. 2(b). As Eq. (8) is essentially the same as the winding number of Eq. (4), the change of the winding

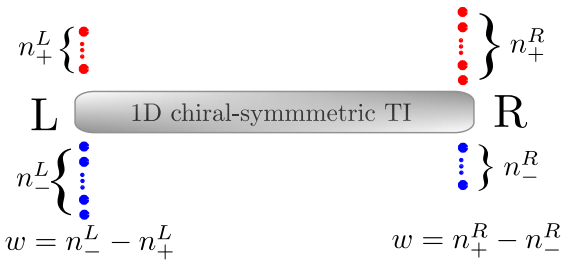

Fig. 3. Hermitian bulk-boundary correspondence in 1D chiral-symmetric topological insulators. The red or blue dots denote zero-energy modes localized at the left or right boundary.

number between L_1 and L_2 equals to the topological invariant of the EP.

V. NON-HERMITIAN BRAIDINGS AND HERMITIAN BULK-BOUNDARY CORRESPONDENCE

According to Hermitian bulk-boundary correspondence, the non-trivial bulk topology corresponds to zero-energy topological boundary states, i.e., $w = n_+^{R(L)} - n_-^{R(L)}$ up to a sign factor. Here, $n_+^{R(L)}$ and $n_-^{R(L)}$ denote the number of zero-energy modes of $|\Psi_+\rangle$ and $|\Psi_-\rangle$ in Eq. (2) that are exponentially localized at the right (left) boundary. Their relation with the bulk non-trivial winding number w is illustrated in Fig. 3.

We have shown that the winding number comes from the non-Hermitian braidings using the linking number of Eq. (5). In one-dimensional non-Hermitian systems, this bulk winding number results in non-Hermitian skin effect (NHSE) [47–51, 54], manifested as the localization of all wavefunctions on boundaries. Note that this phenomenon has been observed recently [52, 53]. As the winding number comes from the linking number, we may regard that the NHSE corresponds to the bulk non-Hermitian braidings.

To further establish the relation between non-Hermitian braidings and Hermitian bulk-boundary correspondence, we show that the NHSE in Q gives rise to topological boundary modes in H following Ref. [51]. Consider a system with NHSE described by $Q^\dagger$ or Q with semi-infinite boundary condition in the left (right) direction. The skin modes are exponentially localized at the right (left) boundary described by $\{E_{i,+}, e^{\alpha j}|\psi_{i,+}\rangle\}$ for $Q^\dagger$ and $\{E_{i,-}, e^{\alpha j}|\psi_{i,-}\rangle\}$ for Q. Here, i is the energy index, j the site index, and α the decaying factor. We focus on the zero modes of $Q^\dagger$ and Q, whose numbers are $n_+^{R(L)}$ and $n_-^{R(L)}$, respectively. Here, the superscript $R(L)$ denotes the right (left) boundary. In constructing H by Q using Eq. (1), owing to Eq. (3), only these zero-energy modes keep the same localization feature as in Q, while all other modes cannot retain in H [60]. This explains the

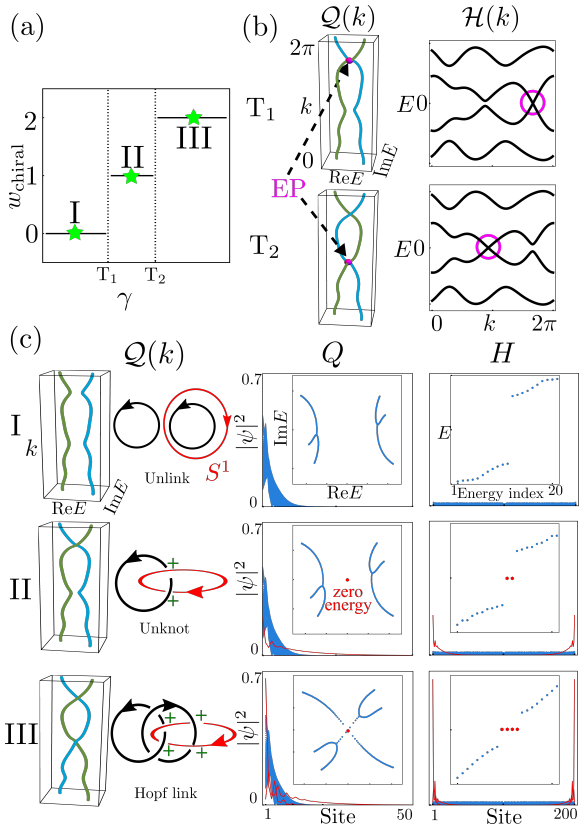

Fig. 4. (a) The phase diagram for both $\mathcal{Q}(k)$ and $\mathcal{H}(k)$ against γ. (b) The correspondence between EPs in non-Hermitian $\mathcal{Q}(k)$ and band crossings (open circle) in Hermitian $\mathcal{H}(k)$. (c) The knots of non-Hermitian bands in the 1D BZ (left panel). The wavefunction profiles of $\mathcal{Q}(k)$ (middle panel) and $\mathcal{H}(k)$ (right panel) with OBC. The insets in the middle panel shows the complex energy spectra of $\mathcal{Q}(k)$ with OBC. The insets in the right panel shows the energy spectra of $\mathcal{H}(k)$ with OBC. The red color refers to zero-energy modes. The parameters are $\Delta = 0.15, g = 3\Delta, \kappa = 1.4\Delta, c = 1.5\Delta$.

non-Hermitian origin of the Hermitian bulk-boundary correspondence in Fig. 3. That is, the topological zero-energy boundary modes in H originate from the zero-energy modes in NHSE of Q, which correspond to the bulk non-Hermitian braidings.

VI. TYPICAL TOPOLOGICAL PHASES WITH NON-HERMITIAN BRAIDINGS

We now proceed to concrete models that demonstrate how the non-Hermitian braidings give rise to Hermitian topological phases as well as their topological boundary states, whose phase transitions are mediated by critical points. Let us consider a double-band $\mathcal{Q}(k)$ with different non-Hermitian braidings, which has been realized recently [59]. The model Hamiltonian reads,

$$\mathcal{Q}(k) = g\sigma_1 + [\kappa\cos k + c\cos(2k) + i\Delta\sin(2k) - i\gamma]\sigma_3. \quad (9)$$

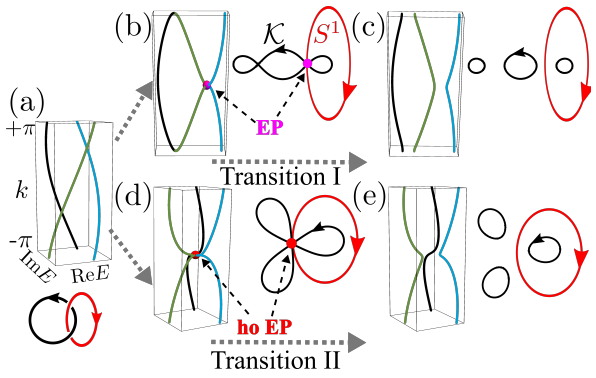

Fig. 5. Generalization to multi-band models with higher-order EPs. Transition I of (a)→(b)→(c) is mediated by order-2 EPs. Here $\alpha = 0$, and $\beta = 0$, 1.89, and 2.2. Transition II of (a)→(d)→(e) is mediated by a higher-order EP (ho EP). Here $\beta = 0$, and $\alpha = 0$, -1, and -1.1.

The two complex-energy eigenvalues are $E(k) = \pm\left([\kappa\cos k + c\cos(2k) + i\Delta\sin(2k) - i\gamma]^2 + g^2\right)^{1/2}$. As shown by I, II, and III in Fig. 4(c) [three green stars in (a)], the braiding of two bands in the $(\mathrm{Re}E(k), \mathrm{Im}E(k), k)$-space leads to different knots (black) in $\mathcal{Q}(k)$. These knots have different linking numbers with the zero-energy loop (red), and thus different phases of $\mathcal{H}(k)$. Specifically, I corresponds to an unlinked phase having zero linking number; II is an unknot phase with linking number $+1$; III is a Hopf link phase with linking number $+2$.

First, we show that the transformation of braiding structure mediated by EPs in $\mathcal{Q}(k)$, as denoted by T_1 and T_2 in Fig. 4(a), leads to Hermitian topological phases transitions in $\mathcal{H}(k)$. Here, $\mathcal{H}((k) = g\sigma_1 \otimes \sigma_1 + [\kappa\cos k + c\cos(2k)]\sigma_1 \otimes \sigma_3 + [\gamma - \Delta\sin(2k)]\sigma_2 \otimes \sigma_3$. We compare the energy spectra of $\mathcal{Q}(k)$ and $\mathcal{H}((k)$ at T_1 and T_2 in Fig. 4(b). The position of band intersection is determined by $E(k) = 0$, as shown by the pink dots in (b). At these points, $\mathcal{Q}(k) = g(\sigma_1 \pm i\sigma_3)$. It is doubly degenerate, but only has one eigenvector of $(\pm i, 1)^T$, corresponding to order-2 EPs. Across these EPs, the winding number changes by $+1$ due to the change of the non-Hermitian braiding. Thus, the Hermitian phase transitions are determined by these critical points.

Second, we demonstrate that the non-Hermitian skin modes with zero energy in $\mathcal{Q}(k)$ result in the topological boundary states of Hermitian $\mathcal{H}(k)$. In the middle panel of Fig. 4(c), the wavefunction profiles of $\mathcal{Q}(k)$ with open boundary conditions (OBC) for I, II, and III phases are plotted, which all possess NHSE. In the right panel of (c), the wavefunction profiles for the corresponding $\mathcal{H}(k)$ are plotted with OBC. We can see that only II and III have topological boundary states. This is because for these two, there are zero-energy skin modes in $\mathcal{Q}(k)$ [red points/curves in (c)], while it is not the case for I [70]. These zero-energy skin modes from $\mathcal{Q}(k)$ survive in $\mathcal{H}(k)$, leading to the topological boundary states.

VII. GENERALIZATION TO MULTI-BAND TOPOLOGICAL PHASES WITH HIGHER-ORDER EPS

The mechanism of non-Hermitian braidings can be generalized to multi-band models where higher-order EPs (ho EPs) may emerge. Here we discuss the case of triple-band $\mathcal{Q}(k)$, where more than two bands could intersect at ho EPs. The non-Hermitian lattice model for $\mathcal{Q}(k)$ reads,

$$\mathcal{Q}(k) = \begin{pmatrix} 0 & \beta & q(k)+\alpha \\ 1 & 0 & 0 \\ 0 & 1 & 0 \end{pmatrix}. \tag{10}$$

Here, $q(k) = \cos k + i\sin k$, and α and β are model parameters. With $\alpha = \beta = 0$, the braiding of the three complex-energy bands forms a knot of circle, as shown in Fig. 5(a). $\mathcal{H}(k)$ possesses a non-trivial phase if zero-energy loop links with this circle.

First, by increasing β, Transition I can be induced as shown by Figs. 5(a,b,c). Similar to Fig. 2, this transition is mediated by order-2 EPs, that is, the intersection of two bands. If one puts the zero-energy loop at such a EP [Fig. 5(b)], the change of knot topology from braiding results in a phase transition. Thus, in multi-band cases, order-2 EPs can still lead to topological phase transitions in $\mathcal{H}(k)$.

Second, by decreasing α, Transition II can be induced as shown by Figs. 5(a,d,e). This transition is mediated by ho EP [red point in (d)]. It is different from Transition I, as there are three bands intersecting at this point. However, ho EP may also mediate topological phase transition. Because by putting zero-energy loop at this point, Transition II also signifies the change of the linking number, resulting the phase transition in $\mathcal{H}(k)$. Therefore, similar to order-2 EPs, ho EP can mediate the change of braiding structure, resulting in the topological phase transitions in $\mathcal{H}(k)$.

VIII. DISCUSSION

We have demonstrated that all the fundamental concepts of chiral-symmetric Hermtian topological phases, including bulk topology, topological phase transition, and bulk-boundary correspondence, have non-Hermitian origins. This non-Hermitian picture provides a deeper understanding which is not possible by Hermitian theories, as signified by the discovery of a novel class of topological phase transitions characterized by the critical points. Hence, our work shows that non-Hermitian topology may be regarded as building blocks of Hermitian topological phases. In view of the rich concepts in non-Hermitian physics, it would be worthwhile to explore further in the following direction. In the case of braiding structures formed by more than two energy bands, similar to the Hermitian systems [71–73], multi-gap(band) conditions may be taken into account. It

is expected that partitioning energy gaps/bands into different groups could lead to different topologies.

[1] J. M. Leinaas and J. Myrheim, Nuovo Cim B **37**, 1 (1977).
[2] F. Wilczek, Phys. Rev. Lett. **48**, 1144 (1982).
[3] C. Nayak, S. H. Simon, A. Stern, M. Freedman, and S. Das Sarma, Rev. Mod. Phys. **80**, 1083 (2008).
[4] Q. Wu, A. A. Soluyanov, and T. Bzdusek, Science **365**, 1273 (2019).
[5] E. Yang, B. Yang, O. You, H.-C. Chan, P. Mao, Q. Guo, S. Ma, L. Xia, D. Fan, Y. Xiang, and S. Zhang, Phys. Rev. Lett. **125**, 033901 (2020).
[6] D. Wang, B. Yang, Q. Guo, R.-Y. Zhang, L. Xia, X. Su, W.-J. Chen, J. Han, S. Zhang, and C. T. Chan, Light Sci Appl **10**, 83 (2021).
[7] H. Park, S. Wong, X. Zhang, and S. S. Oh, ACS Photonics **8**, 2746 (2021).
[8] A. Bouhon, Q. Wu, R.-J. Slager, H. Weng, O. V. Yazyev, and T. Bzdusek, Nat. Phys. **16**, 1137 (2020).
[9] Q. Guo, T. Jiang, R.-Y. Zhang, L. Zhang, Z.-Q. Zhang, B. Yang, S. Zhang, and C. T. Chan, Nature **594**, 195 (2021).
[10] B. Jiang, A. Bouhon, Z.-K. Lin, X. Zhou, B. Hou, F. Li, R.-J. Slager, and J.-H. Jiang, Nat. Phys. **17**, 1239 (2021).
[11] B. Peng, A. Bouhon, B. Monserrat, and R.-J. Slager, Nat Commun **13**, 423 (2022).
[12] Z. Yang, C.-K. Chiu, C. Fang, and J. Hu, Phys. Rev. Lett. **124**, 186402 (2020).
[13] W. Tang, X. Jiang, K. Ding, Y.-X. Xiao, Z.-Q. Zhang, C. T. Chan, and G. Ma, Science **370**, 1077 (2020).
[14] K. Wang, L. Xiao, J. C. Budich, W. Yi, and P. Xue, Phys. Rev. Lett. **127**, 026404 (2021).
[15] W. Tang, K. Ding, and G. Ma, arXiv:2112.00982 (2021).
[16] D.-L. Deng, S.-T. Wang, C. Shen, and L.-M. Duan, Phys. Rev. B **88**, 201105 (2013).
[17] T. c. v. Bzdušek and M. Sigrist, Phys. Rev. B **96**, 155105 (2017).
[18] J. Ahn, D. Kim, Y. Kim, and B.-J. Yang, Phys. Rev. Lett. **121**, 106403 (2018).
[19] K. Wang, J.-X. Dai, L. B. Shao, S. A. Yang, and Y. X. Zhao, Phys. Rev. Lett. **125**, 126403 (2020).
[20] K. Esaki, M. Sato, K. Hasebe, and M. Kohmoto, Phys. Rev. B **84**, 205128 (2011).
[21] D. Leykam, K. Y. Bliokh, C. Huang, Y. D. Chong, and F. Nori, Phys. Rev. Lett. **118**, 040401 (2017).
[22] Y. Xiong, J. Phys. Commun. **2**, 035043 (2018).
[23] H. Menke and M. M. Hirschmann, Phys. Rev. B **95**, 174506 (2017).
[24] Y. Xu, S.-T. Wang, and L.-M. Duan, Phys. Rev. Lett. **118**, 045701 (2017).
[25] T. E. Lee, Phys. Rev. Lett. **116**, 133903 (2016).
[26] H. Shen, B. Zhen, and L. Fu, Phys. Rev. Lett. **120**, 146402 (2018).
[27] H. Zhou, C. Peng, Y. Yoon, C. W. Hsu, K. A. Nelson, L. Fu, J. D. Joannopoulos, M. Soljačić, and B. Zhen, Science **359**, 1009 (2018).
[28] W. B. Rui, Z. Zheng, M. M. Hirschmann, S.-B. Zhang, C. Wang, and Z. D. Wang, npj Quantum Mater. **7**, 15 (2022).
[29] J. Hou, Z. Li, X.-W. Luo, Q. Gu, and C. Zhang, Phys. Rev. Lett. **124**, 073603 (2020).
[30] Z. Gong, Y. Ashida, K. Kawabata, K. Takasan, S. Higashikawa, and M. Ueda, Phys. Rev. X **8**, 031079 (2018).
[31] W. B. Rui, M. M. Hirschmann, and A. P. Schnyder, Phys. Rev. B **100**, 245116 (2019).
[32] K. Kawabata, K. Shiozaki, M. Ueda, and M. Sato, Phys. Rev. X **9**, 041015 (2019).
[33] L. Li, C. H. Lee, and J. Gong, Phys. Rev. B **100**, 075403 (2019).
[34] E. J. Bergholtz, J. C. Budich, and F. K. Kunst, Rev. Mod. Phys. **93**, 015005 (2021).
[35] M. Berry, Czechoslovak Journal of Physics **54**, 1039 (2004).
[36] W. D. Heiss, J. Phys. A: Math. Theor. **45**, 444016 (2012).
[37] M.-A. Miri and A. Alu, Science **363**, eaar7709 (2019).
[38] T. Kato, in *Perturbation Theory for Linear Operators*, Classics in Mathematics, edited by T. Kato (Springer, Berlin, Heidelberg, 1995) pp. 62–126.
[39] K. Kawabata, T. Bessho, and M. Sato, Phys. Rev. Lett. **123**, 066405 (2019).
[40] W. B. Rui, Y. X. Zhao, and A. P. Schnyder, Phys. Rev. B **99**, 241110 (2019).
[41] D. Bernard and A. LeClair, in *Statistical Field Theories*, NATO Science Series, edited by A. Cappelli and G. Mussardo (Springer Netherlands, Dordrecht, 2002) pp. 207–214.
[42] H. Zhou and J. Y. Lee, Phys. Rev. B **99**, 235112 (2019).
[43] S. Lieu, Phys. Rev. B **98**, 115135 (2018).
[44] J. C. Budich, J. Carlström, F. K. Kunst, and E. J. Bergholtz, Phys. Rev. B **99**, 041406 (2019).
[45] W. B. Rui, Z. Zheng, C. Wang, and Z. D. Wang, Phys. Rev. Lett. **128**, 226401 (2022).
[46] C. H. Lee and R. Thomale, Phys. Rev. B **99**, 201103 (2019).
[47] F. K. Kunst, E. Edvardsson, J. C. Budich, and E. J. Bergholtz, Phys. Rev. Lett. **121**, 026808 (2018).
[48] S. Yao and Z. Wang, Phys. Rev. Lett. **121**, 086803 (2018).
[49] K. Yokomizo and S. Murakami, Phys. Rev. Lett. **123**, 066404 (2019).
[50] K. Zhang, Z. Yang, and C. Fang, Phys. Rev. Lett. **125**, 126402 (2020).
[51] N. Okuma, K. Kawabata, K. Shiozaki, and M. Sato, Phys. Rev. Lett. **124**, 086801 (2020).
[52] L. Xiao, T. Deng, K. Wang, G. Zhu, Z. Wang, W. Yi, and P. Xue, Nat. Phys. **16**, 761 (2020).
[53] T. Helbig, T. Hofmann, S. Imhof, M. Abdelghany, T. Kiessling, L. W. Molenkamp, C. H. Lee, A. Szameit, M. Greiter, and R. Thomale, Nat. Phys. **16**, 747 (2020).
[54] D. S. Borgnia, A. J. Kruchkov, and R.-J. Slager, Phys. Rev. Lett. **124**, 056802 (2020).
[55] Z. Li and R. S. K. Mong, Phys. Rev. B **103**, 155129 (2021).
[56] C. C. Wojcik, X.-Q. Sun, T. Bzdušek, and S. Fan, Phys. Rev. B **101**, 205417 (2020).
[57] H. Hu and E. Zhao, Phys. Rev. Lett. **126**, 010401 (2021).
[58] H. Hu, S. Sun, and S. Chen, arXiv:2111.11346 (2021).

[59] K. Wang, A. Dutt, C. C. Wojcik, and S. Fan, Nature **598**, 59 (2021).

[60] Away from zero energy, the eigenequation can also be obtained by the non-Hermitian components Q and $Q^\dagger$, i.e., $Q\psi_- = E\psi_+$ and $Q^\dagger\psi_+ = E\psi_-$, which yield $QQ^\dagger\psi_+ = E^2\psi_+$, $Q^\dagger Q\psi_- = E^2\psi_-$. However, this becomes a coupled eigenvalue problem, and the information from either Q or $Q^\dagger$ alone cannot be retained in the Hermitian Hamiltonian H.

[61] C.-K. Chiu, J. C. Y. Teo, A. P. Schnyder, and S. Ryu, Rev. Mod. Phys. **88**, 035005 (2016).

[62] A. J. Heeger, S. Kivelson, J. R. Schrieffer, and W. P. Su, Rev. Mod. Phys. **60**, 781 (1988).

[63] J. K. Asbóth, L. Oroszlány, and A. Pályi, in *A Short Course on Topological Insulators: Band Structure and Edge States in One and Two Dimensions*, Lecture Notes in Physics, edited by J. K. Asbóth, L. Oroszlány, and A. Pályi (Springer International Publishing, Cham, 2016) pp. 1–22.

[64] R. Roy and F. Harper, Phys. Rev. B **96**, 155118 (2017).

[65] J. Y. Lee, J. Ahn, H. Zhou, and A. Vishwanath, Phys. Rev. Lett. **123**, 206404 (2019).

[66] Given non-Hermitian Q_1 and Q_2, they have the same point-gap topology about a refence point E_P on the complex-energy plane, if their spectra can be smoothly deformed to each other without crossing E_P.

[67] Here, the simplification refers to the comparison between integration and counting crossings. There might be another computational cost arising in calculating the linking number. That is, to obtain the linking number, it is required to identify all the eigenvalues, while in Eq. (4) only the computation of the determinant is required..

[68] Z. Yang, A. P. Schnyder, J. Hu, and C.-K. Chiu, Phys. Rev. Lett. **126**, 086401 (2021).

[69] See the Supplemental Material for details.

[70] We note that in Q, the zero-energy modes themselves in Fig. 4(c) II and III are skin modes, not topological boundary modes. After constructing H by Q, they become topological modes. See supplemental material for details.

[71] A. Bouhon, T. c. v. Bzdušek, and R.-J. Slager, Phys. Rev. B **102**, 115135 (2020).

[72] F. N. Ünal, A. Bouhon, and R.-J. Slager, Phys. Rev. Lett. **125**, 053601 (2020).

[73] A. Bouhon and R.-J. Slager 10.48550/arXiv.2203.16741 (2022).